J. ENVIRONMENTAL SYSTEMS, Vol. 24(3) 241-262, 1995-96

MODELING OF SEWAGE CIRCULATING REACTOR: AN APPROACH TO RECIRCULATING WASTEWATER IN SEWERS

UTTAM K. MANANDHAR

HANS SCHRODER

SERD, Asian Institute of Technology, Thailand

ABSTRACT

One way to exploit the self-purifying capacity of flowing wastewater is to recirculate it so that a portion of the conveyance conduit works as a circulating biological reactor (referred to as a Sewage Circulating Reactor, SCR). This study deals with the formulation of a mathematical model for this system based on suspended-growth and biofilm kinetics. The model simulated the performance of the system satisfactorily and showed that all three biological reactions, carbon oxidation, nitrification, and denitrification, occurred simultaneously in the system. The model simulation also indicated that both suspended and film biomasses were significant at low loadings in terms of organic carbon removal. At higher loadings, suspended biomass was more significant than biofilm biomass for COD removal. The maximum substrate utilization rates (K_m values) for carbon oxidation, nitrification, and denitrification were obtained by fitting simulated profiles with the experimental ones. The k_m values for carbon oxidation and nitrification were higher for experimental runs with higher DO levels or lower loadings. However, the K_m value for denitrification was higher for the case of higher loadings.

INTRODUCTION

All biological treatment systems in general use contain suspended and attached-growth biomass for biological treatment of wastewater. The same kind of processes (referred as self-purification) are active in sewers. This is true for open channels as well as closed conduits.

doi: 10.2190/RK6Y-L3GB-847W-U1JW
http://baywood.com

A 37 km. looped-shaped sewerage system in Tel Aviv, Israel employing an aerobic step-fed plug flow reactor [1], pressure pipe wastewater treatment [2], and the use of pipelines as aerobic biological reactors [3], indicates the potential of sewer systems to be used as treatment reactors.

One way to exploit the self-purifying capacity of sewer systems is to recycle the wastewater back to its starting point, so using a portion of conveyance channel or conduit as a biological reactor, hereafter termed a Sewage Circulating Reactor [4]. This approach is applicable in small communities, industrial estates, and rural areas with looped sewerage systems. In our research, a mathematical model is formulated based on suspended and attached growth kinetics to simulate the overall performance of this system.

Pilot-scale experimental results obtained with synthetic wastewater described elsewhere [4] are used to confirm the mathematical model. Then the model is used to investigate the active mechanisms at work in the system. The experimental conditions are summarized in Table 1.

Table 1. Operating Conditions for Experimental Runs

	Run Number					
Description	S1	S2	S3	S4	S5	S6
Influent Flow (m^3/h)	0.36	0.36	0.36	0.36	0.36	0.36
Recirculation Ratio	52.7	27.9	52.7	52.7	27.9	52.7
Flow Velocity (m/s)	0.38	0.33	0.35	0.43	0.39	0.47
	-0.60	-0.56	-0.62	-0.59	-0.50	-0.64
Flow Depth (m)	9.8-	6.3-	10.8-	11.8-	7.1-	9.83
	13.3	8.79	18.7	15.6	8.5	-13.23
COD Loading Rate						
Areal ($g/m^2/d$)	16.81	20.14	27.45	41.95	47.15	62.02
Volume ($kg/m^3/d$)	0.56	0.77	0.86	1.34	1.76	2.07
TN Loading Rate						
Areal ($g/m^2/d$)	1.8	2.54	3.78	5.14	6.41	7.84
Volume ($kg/m^3/d$)	0.06	0.10	0.12	0.16	0.24	0.26
Influent COD (mg/L)	55.26	46.85	110.60	158.0	115.60	200.00
Influent NH_3-N (mg/L)	5.44	5.40	14.98	18.88	15.46	24.63
HRT (h)	2.7	1.5	2.7	2.7	1.5	2.7

MATHEMATICAL MODEL

The Sewage Circulating Reactor consisted of an 87.12 m long channel of dimensions 0.08 × 0.20 (width × depth) with an average bed slope of 0.4 percent, within the normal range of gravity sewers' bed slope. The wastewater was recirculated back to the starting point by means of a centrifugal pump through a recirculation tank. Details about the set-up and experimental works can be found in [4].

Since the dissolved oxygen (DO) level decreased along the channel, it was hypothesized that simultaneous carbon oxidation, nitrification, and denitrification occurred in the Sewage Circulating Reactor (SCR).

The constant substrate concentration profiles along the channel suggest that the performance of SCR approached that of completely-mixed conditions due to high recycle flow. However, the hydraulic pattern along the channel is plug-flow with effluent recirculation. Therefore, the SCR is hydraulically represented by many segments (plug-flow reactors) connected in series with effluent recycling. The DO in the system achieved a distinct and stable profile depending on loadings. Bulk substrate concentrations control their fluxes into bio-slimes, and hence different biochemical reactions occur in plug flow reactors based on different bulk substrate concentrations. The model is formulated in such a way that length of each plug-flow reactor can be chosen appropriately. In this study, the SCR was divided into thirty plug-flow reactors connected in series, out of which the first twenty-nine have a length of 3 m and the last one 0.12 m. In addition, the recirculation tank is modelled as a continuously stirred tank reactor. The flow diagram of SCR is shown in Figure 1.

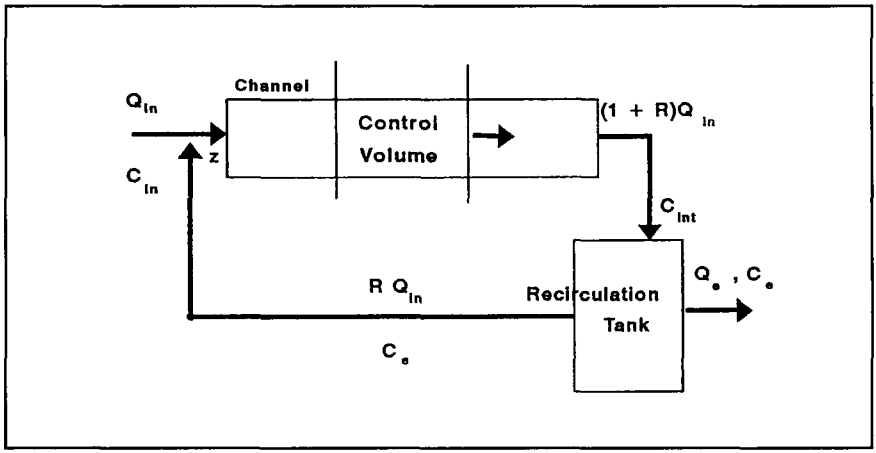

Figure 1. Flow diagram of SCR.

Assumptions in the SCR model are that: 1) longitudinal dispersion effects and vertical gradient of substrate concentration over the cross section are insignificant; 2) the change in substrate concentrations in a plug-flow reactor (segment of channel) is small enough so that the influent concentrations to that reactor can be considered as the average value for that segment; 3) low concentration of organic carbon in the system due to high recirculation ratio makes the competition between nitrifiers and heterotrophs possible, thus causing concurrent carbon oxidation and nitrification; 4) denitrification also occurs simultaneously due to continuously decreasing DO profile and the anoxic zone within deep biofilms; 5) all three species of bacteria, i.e., heterotrophs, nitrifiers, and denitrifiers exist uniformly in the whole biofilm such that the sum of all bacteria serves as a metabolic unit and carries out oxidation, nitrification, and denitrification simultaneously [5]; 6) the channel velocity is high enough to promote detachment of excessive biofilm as well as to avoid sedimentation of suspended solids along the channel; 7) the liquid sublayer thickness (L_l), used to represent external mass transport resistance is determined from the energy dissipation rate, ε in the liquid [6], as $L_l = (\varepsilon/\upsilon^3)^{-1/4}$; 8) the energy dissipation rate, ε calculated as depth average value is given by $\theta g\bar{U}(1 + 2H/W)^{-1}$; 9) a single substrate, either electron donors (COD and NH_3-N) or electron acceptor (NO_x-N and O_2) is limiting with biofilms; 10) diffusion of substrate in the direction of flow of bulk liquid within the bulk liquid is negligible in comparison to transport by advection; and 11) transport of substrate through the liquid sublayer and biofilm is by molecular diffusion.

Model Formulation

Considering the control volume, and the main mechanisms (advective transport and biochemical reactions) within it as shown in Figures 1 and 2 respectively, the mass balance for the substrate in the control volume can be written as,

$$\Delta v \frac{dc}{dt} = QC - \left[QC + \frac{\partial(QC)}{\partial x} \Delta x \right] - \Delta V \cdot r_s - A_s \cdot J_c \qquad (1)$$

At steady-state, the mass balance equation reduces to the following form:

$$U \frac{dc}{dx} = - r_s - a \cdot J_c \qquad (2)$$

Simultaneous carbon oxidation, nitrification, and denitrification is occurring in the bulk liquid together with diffusion of substrates into the biofilm and advection along the channel. These biochemical reactions are concurrently taking place within the biofilm depending on the diffusion fluxes and prevailing concentrations of these substrates within the biofilm. These metabolic activities and interactions between them are schematically shown in Figure 3. This substrate utilization by suspended biomass involves many mechanisms as shown in Figure 3. The rate, r_s

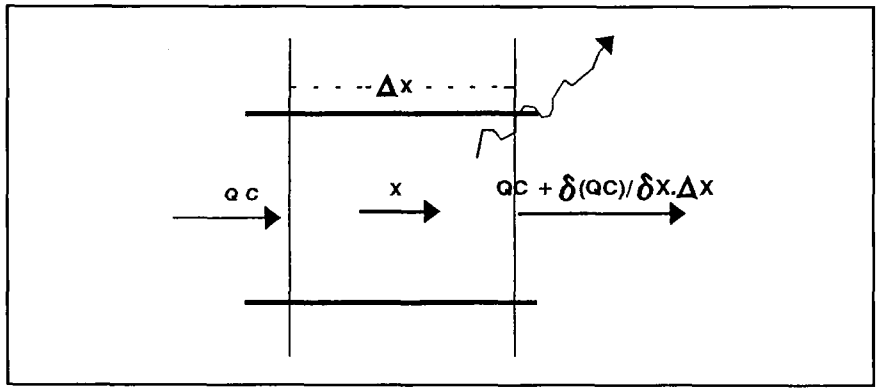

Figure 2. Control volume.

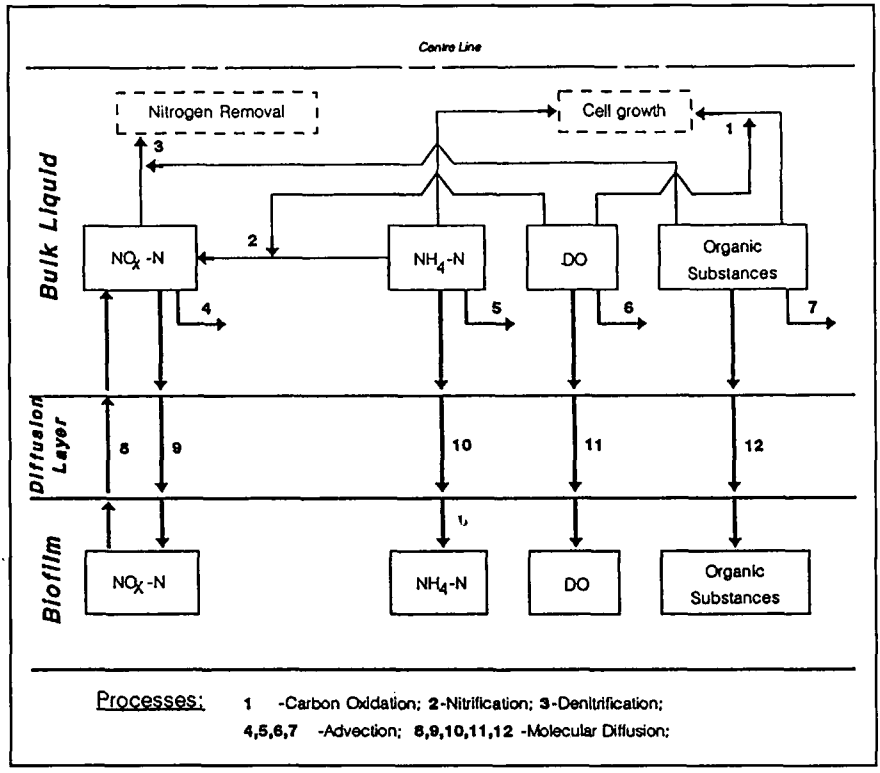

Figure 3. Conceptual representation of biochemical reactions and transport processes in the control volume.

correspondingly involves many terms in the mass balance equations (similar to Eq. 2) for COD, ammonia nitrogen, and oxidized nitrogen (NO_x-N).

Mass balance for ammonium nitrogen consists of loss due to nitrification in bulk liquid, transport by advection, and diffusion into biofilm corresponding to nitrification and cell synthesis. Therefore, the mass balance equation for ammonium nitrogen is,

$$U\frac{dN}{dx} = -\frac{K_{msn}N}{K_{sn}+N}\frac{O}{K_{son}+O}X - aJ_n - afJ_s \tag{3a}$$

Oxidized nitrogen is transported by advection, produced by nitrification, and removed by denitrification in bulk liquid. NO_x-N also diffuses into the biofilm corresponding to the occurrence of denitrification within biofilm, and NO_x-N formed by nitrification within biofilm diffuses out to bulk liquid. Thus, mass balance for oxidized nitrogen will be,

$$U\frac{dP}{dx} = -\frac{K_{msp}P}{K_{sp}+P}\frac{S}{K_{ssp}+S}\frac{K_{sor}}{K_{sor}++O}X + \frac{K_{msn}N}{K_{sn}+N}\frac{O}{K_{son}+O}X - aJ_p + aJ_n \tag{3b}$$

Besides advection, COD is consumed during oxidation and denitrification in bulk liquid, and diffuses into biofilm corresponding to carbon oxidation and denitrification within biofilm. Therefore, the mass balance for COD is:

$$U\frac{dS}{dx} = -\frac{K_{mss}S}{K_{sss}+S}\frac{O}{K_{sos}+O}X - \beta\frac{K_{msp}P}{K_{sp}+P}\frac{S}{K_{ssp}+S}\frac{K_{sor}}{K_{sor}+O}X - aJ_s - \beta aJ_p \tag{3c}$$

To obtain mass fluxes of these substrates into the biofilm, it must be known which of the biochemical reactions (carbon oxidation, nitrification, and denitrification) are occurring within the biofilm. This is determined on the basis of penetration depths [7] of these substrates as explained elsewhere [8]. Then, for biochemical reactions occurring in the biofilm, mass fluxes of substances are calculated by a pseudoanalytical steady-state biofilm model [9]. For this, the flux limiting component (electron donor or acceptor) is taken as the limiting component and determined as explained in [10] and in greater detail in [8].

Solution Technique

The influent concentrations (NH_4-N, NO_x-N, COD) are input values. The concentrations of these substrates in the recycle are set at zero in the first iteration.

Therefore, the input concentrations of these substrates to the reactor are calculated by considering the mass balance of these substrates at the junction between inflow and recycle (i.e., at point Z in Figure 1). For ammonia nitrogen, this is given by,

$$N^{it+1} = \frac{Q_{in}N_{in} + RQ_{in} \cdot N_e^{it}}{(1+R)\,Q_{in}} \tag{4}$$

Similar equations can be written for steady-state NO_x-N and COD concentrations at a point Z (i.e., for P^{it+1}, S^{it+1} respectively). Mass balance equations (Eqs. 3a-3c) are numerically solved by using the Adaptive Runge-Kutta method. This is done for all plug-flow reactors till the whole channel length is covered; the fluxes J_n, J_p, and J_s being obtained each time as explained earlier.

Next, the recirculation tank is modeled as a continuously stirred tank reactor. Steady-state mass balance for the substrates in the tank (i.e., accumulation = input - output + sources - sinks = 0) gives a set of nonlinear equations. The recycled water qualities (i.e., S_e, N_e, and P_e) are obtained by solving this set of nonlinear equations by Brown's method [11].

Thus the simulated effluent concentrations for this particular iteration are obtained and compared with the previous iteration values. The whole operation is repeated till the convergence criteria are met, as in Figure 4.

Model Calibration

The main objective of the model simulation was to describe performance of the system together with main mechanisms occurring in it. The general convergence criteria would be to have sufficiently negligible difference in all three effluent water quality parameters between two consecutive iterations. However, this could not always be obtained due to interactions between these substrates; e.g., denitrification decreased both NO_x-N and COD. Therefore, a stringent steady state condition was imposed on one of these substrates as compared to the other two. Accordingly, the convergence criteria used in all model simulations was that values of e_1, e_2 and e_3 in simulation flow chart (Figure 4) were 3.0, 3.0, and 0.1 percent, respectively. This was chosen because of the fact that values less than these did not produce any significant difference in the model results.

All kinetic coefficients, other than the maximum substrate utilization rates (i.e., half saturation constants, yield coefficients, decay constants) are adopted from literature, and stoichiometric ratios are taken based on stoichiometry of biological reactions [12]. These values are given in Table 2.

Since rate constants for biological reactions are specific to environmental conditions and maximum substrate utilization rates are significant, these rates for biofilms and suspended biomass were calibrated by fitting the simulated profiles with experimental ones. The first three (i.e., runs S1 to S3) of total six runs of experiments with synthetic wastewater seemed to have a different performance compared to the other three (S4 or S6) in terms of COD, NH_3-N, NO_x-N, and DO

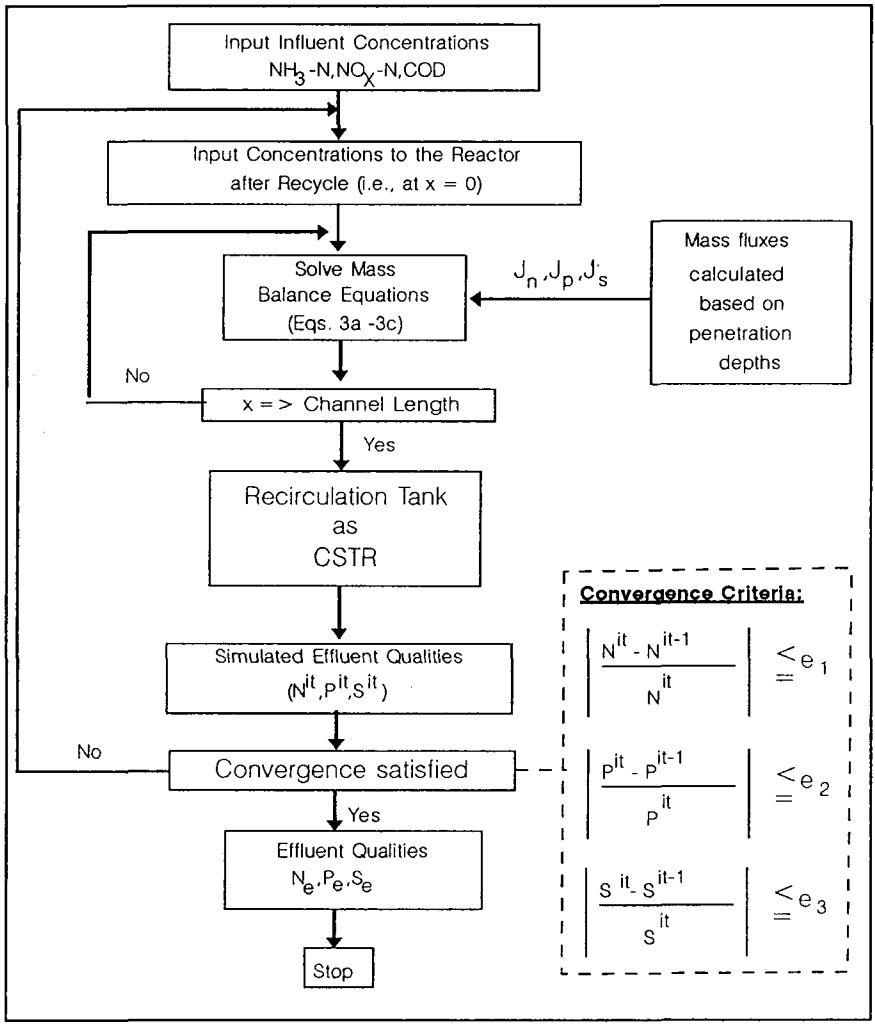

Figure 4. Flow chart for simulation.

levels. Therefore, these maximum rates were calibrated separately for these two situations choosing runs S2 and S4 for these two cases respectively. Fitting between simulated and experimental profiles is shown graphically in Figures 5 (run S2) and 6 (run S4). The maximum rates thus obtained are summarized in Table 3. The maximum substrate utilization rates of carbon oxidation and nitrification were higher for run S2 than for run S4. On the other hand, the maximum substrate utilization rate of denitrification was higher for run S4.

Table 2. Values of Kinetic and Stoichiometric Coefficients

Description	Value	Reference
D_{ws}	5.8×10^{-5} m²/d	7
D_{wn}	1.5×10^{-4} m²/d	10
D_{wp}	1.4×10^{-4} m²/d	10
D_{wo}	2.2×10^{-4} m²/d	10
D_{fs}	2.3×10^{-5} m²/d	7
D_{fn}	1.1×10^{-4} m²/d	13
D_{fp}	1.3×10^{-4} m²/d	10
D_{fo}	1.7×10^{-4} m²/d	13
K_{fn}	1.4 mg N/L	14
K_{fon}	0.1 mg/L	15
K_{fp}	0.1 mg N/L	14
K_{fsp}	1.5 mg COD/L	15
K_{fss}	20.0 mg COD/L	5
K_{fos}	0.2 mg/L	5
K_{sn}	3.59 mg N/L	16
K_{son}	0.63 mg/L	16
K_{sos}	0.2 mg/L	5
K_{sss}	20.0 mg COD/L	5
Y_1	0.4 mg VSS/mgCOD	14
Y_2	0.2 mg VSS/mg N	14
Y_{1d}	0.8 mg VSS/mg N	14
b_1	0.06 1/d	14
b_2	0.05 1/d	14
b_{1d}	0.04 1/d	14
f	0.06	Based on Stoichiometry (12)
f_{oc}	0.36	
f_{oa}	4.06	

Model Validation

The maximum substrate utilization rates obtained in Table 3 were used to calculate performances of other runs (runs S1, S3, S5, S6). Run S1 performance was simulated with coefficients from Run S2, and coefficients from Run S4 were used to simulate runs S5 and S6. These are shown in Figures 7, 8, and 9. The experimental COD and ammonia nitrogen profiles fitted well for run S1 as compared to NO_x-N profile. For run S5, all these profiles fitted reasonably well. In case of run S6, simulated ammonia nitrogen and NO_x-N profiles fitted well with experiments although the COD profile deviated somewhat.

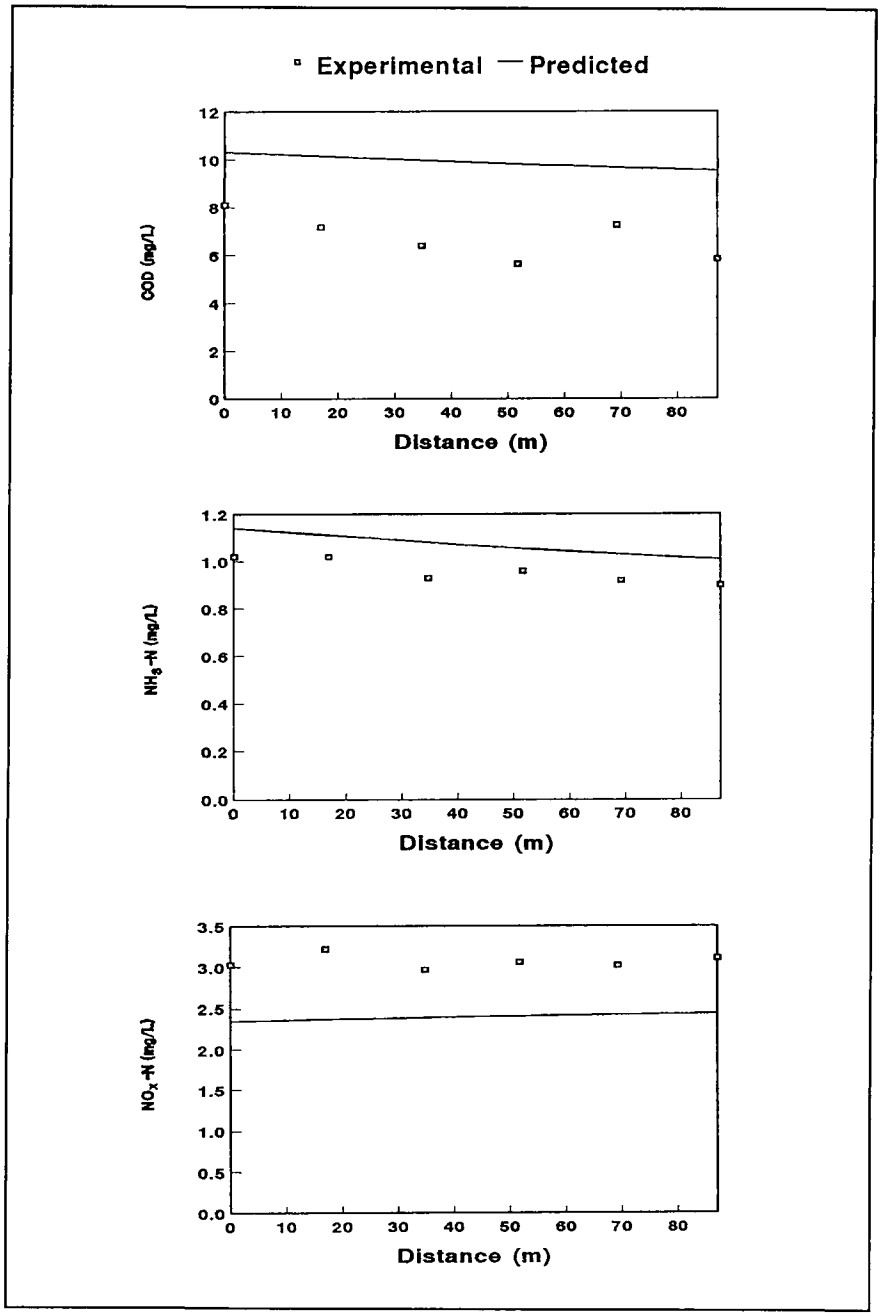

Figure 5. Fitted profiles for Run S2.

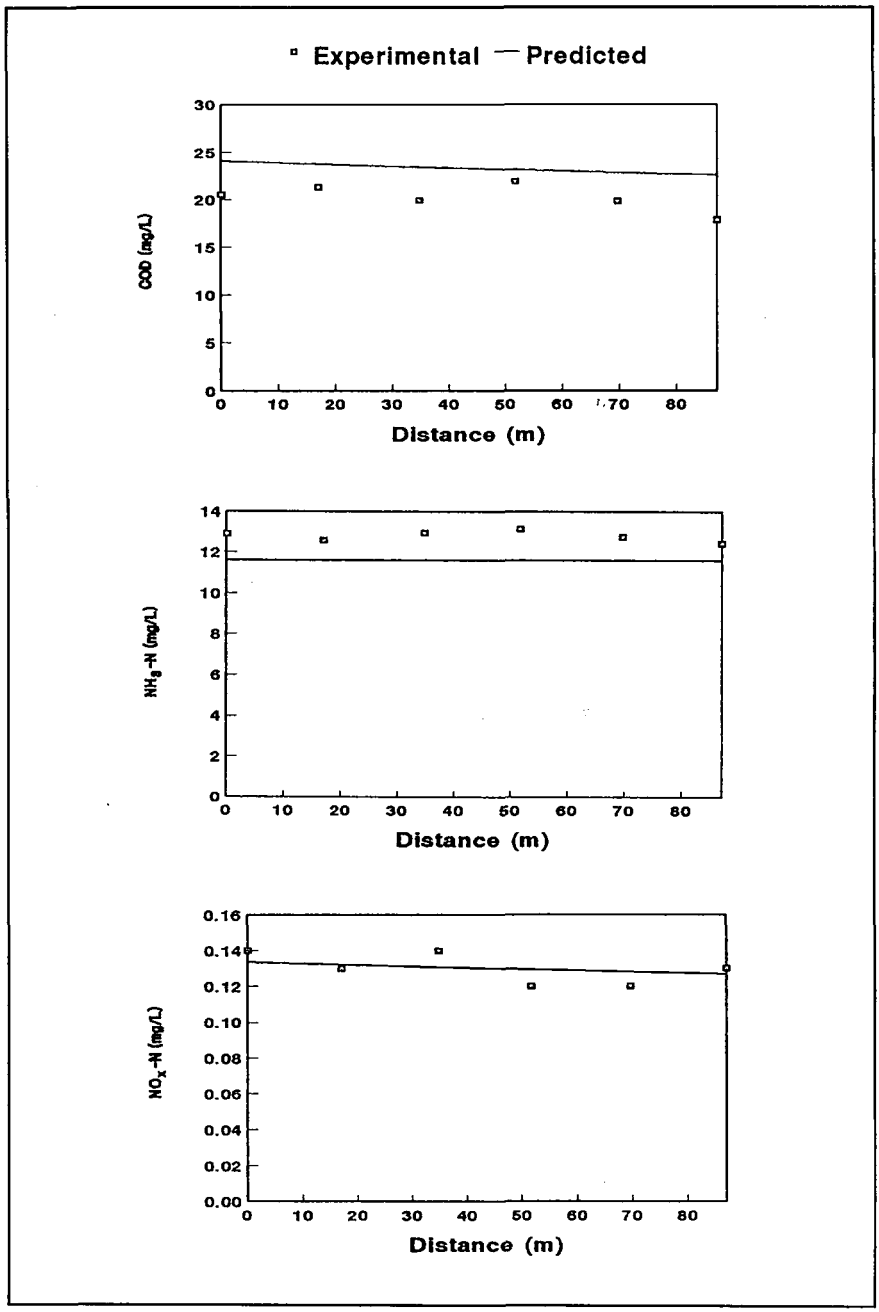

Figure 6. Fitted profiles for Run S4.

Table 3. Maximum Rates for Attached and Suspended Biomass

	Value (1/d)			
	Run S2		Run S4	
Description	Ambient Temp	20°C	Ambient Temp	20°C
For Biofilms				
K_{mfs}	50.15	21.51	28.15	12.07
K_{mfn}	2.9	1.24	0.25	0.11
K_{mfp}	0.03	0.02	2.18	1.28
For Suspended Biomass				
K_{mss}	58.15	24.94	46.15	19.79
K_{msn}	3.68	1.58	0.02	0.01

Run S3 was simulated by using maximum substrate utilization rates determined from run S2 and S4 separately. These are shown in Figure 10. It can be seen that simulations deviated very much from experimental profiles in either case as compared to those for other runs. This was due to the fact that runs S4 and S6 represented the case of complete denitrification, with high denitrification rate and low nitrification rate, whereas runs S1 and S2 simulated the case of complete nitrification with less denitrification. Run S3 corresponded to the transition between these two cases, with incomplete nitrification due to limiting DO [17], since the NO_2-N level was as high as that of runs S1, S2, and NO_3-N level was relatively low.

The model simulation also gives the performance of the system in terms of type of reactions taking place within biofilms and the limiting component for each reaction. The simulation showed that runs S1 and S2 had similar conditions within the biofilms all along the channel. All three types of reactions (carbon oxidation, nitrification, and denitrification) occurred within biofilms all along channel; the limiting component being donor. On the other hand, runs S4, S5, and S6 reflected similar situations. In all these runs, all three types of reactions occurred with donor being limiting component for carbon oxidation and acceptor being limiting component for nitrification and denitrification.

Contribution of Suspended and Biofilm Biomasses

The effect of the suspended biomass on substrate utilization was determined by setting the specific surface area, a in Equations 3a to 3c equal to zero. Similarly, with maximum substrate utilization rates K_{msn}, K_{msp}, and K_{mss} being set to zero in

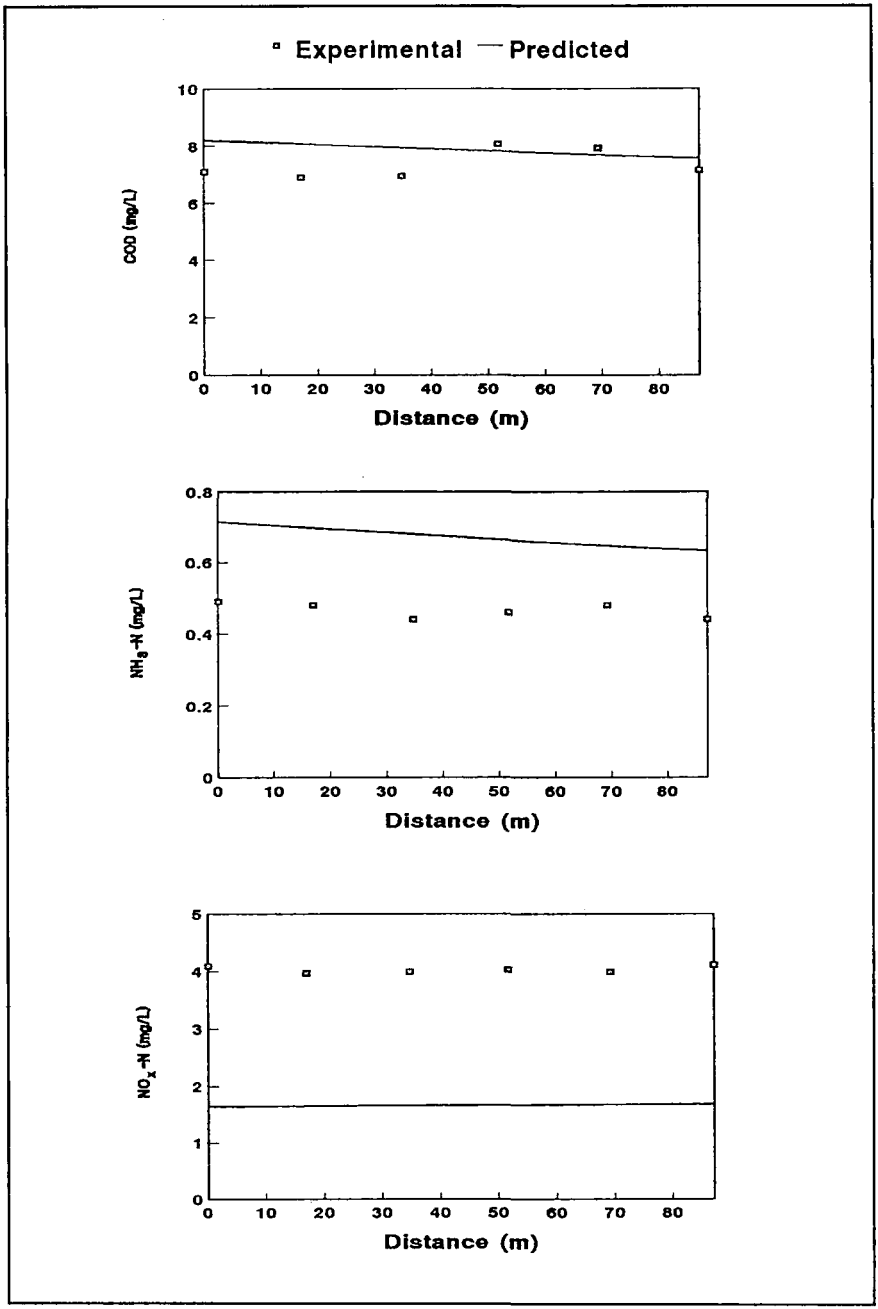

Figure 7. Simulated profiles for Run S1.

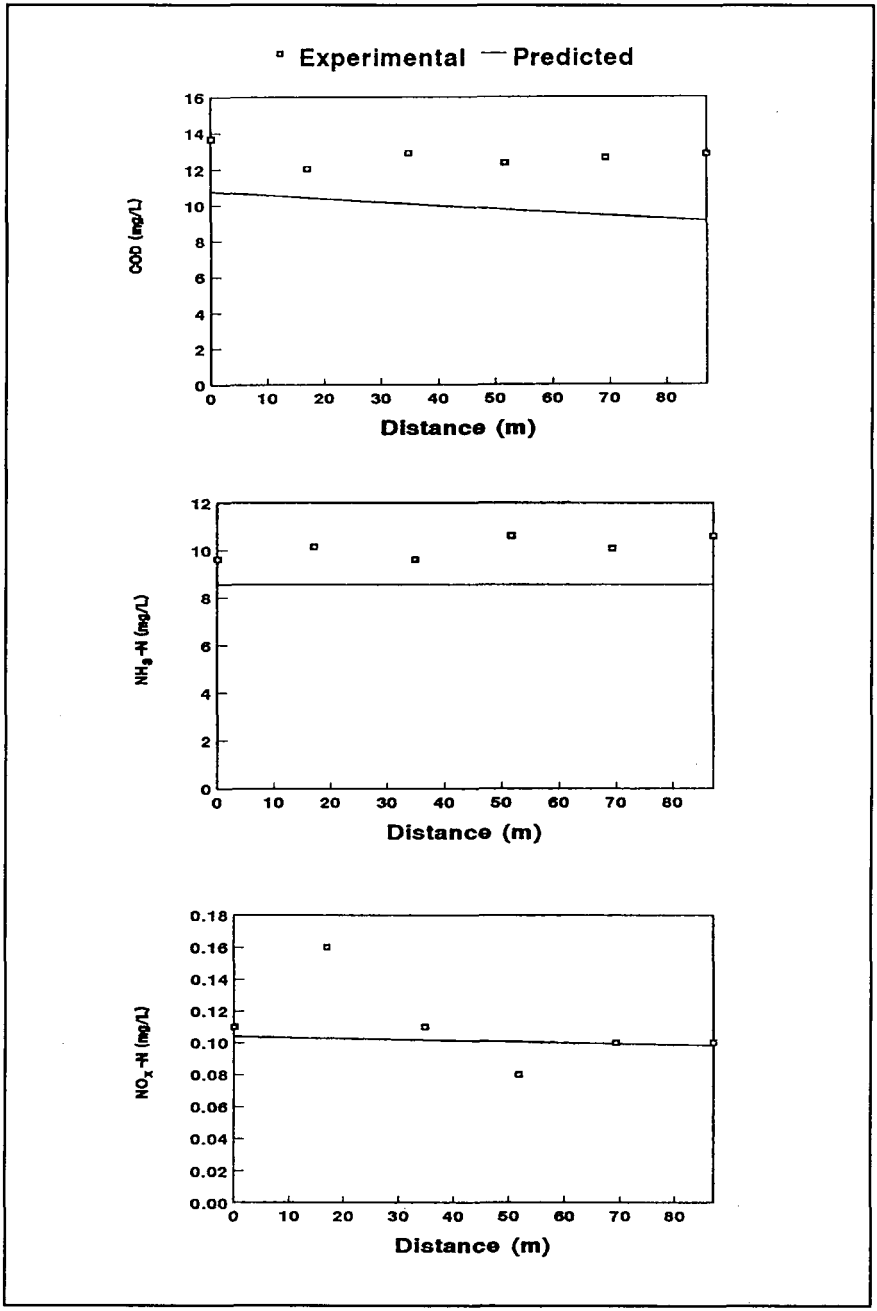

Figure 8. Simulated profiles for Run S5.

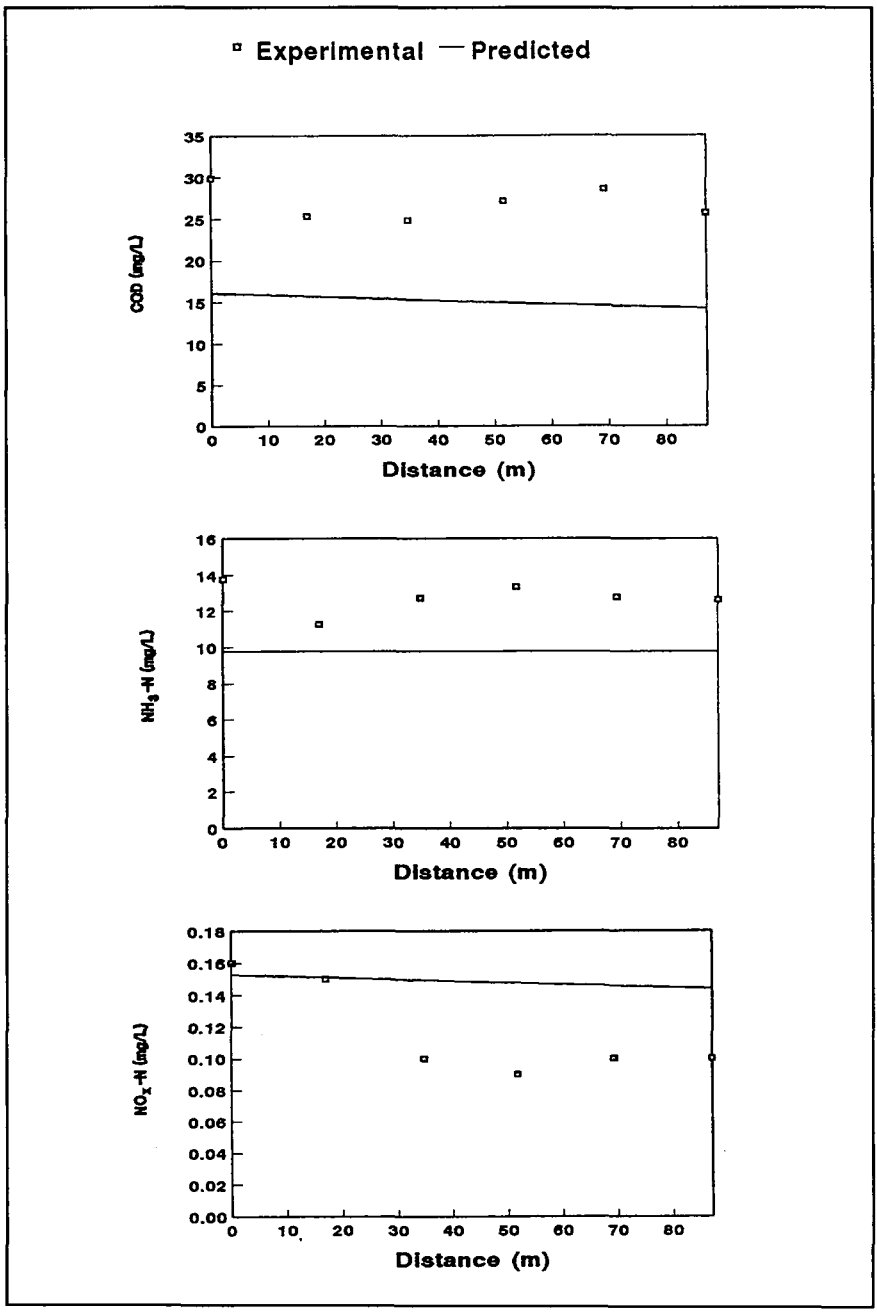

Figure 9. Simulated profiles for Run S6.

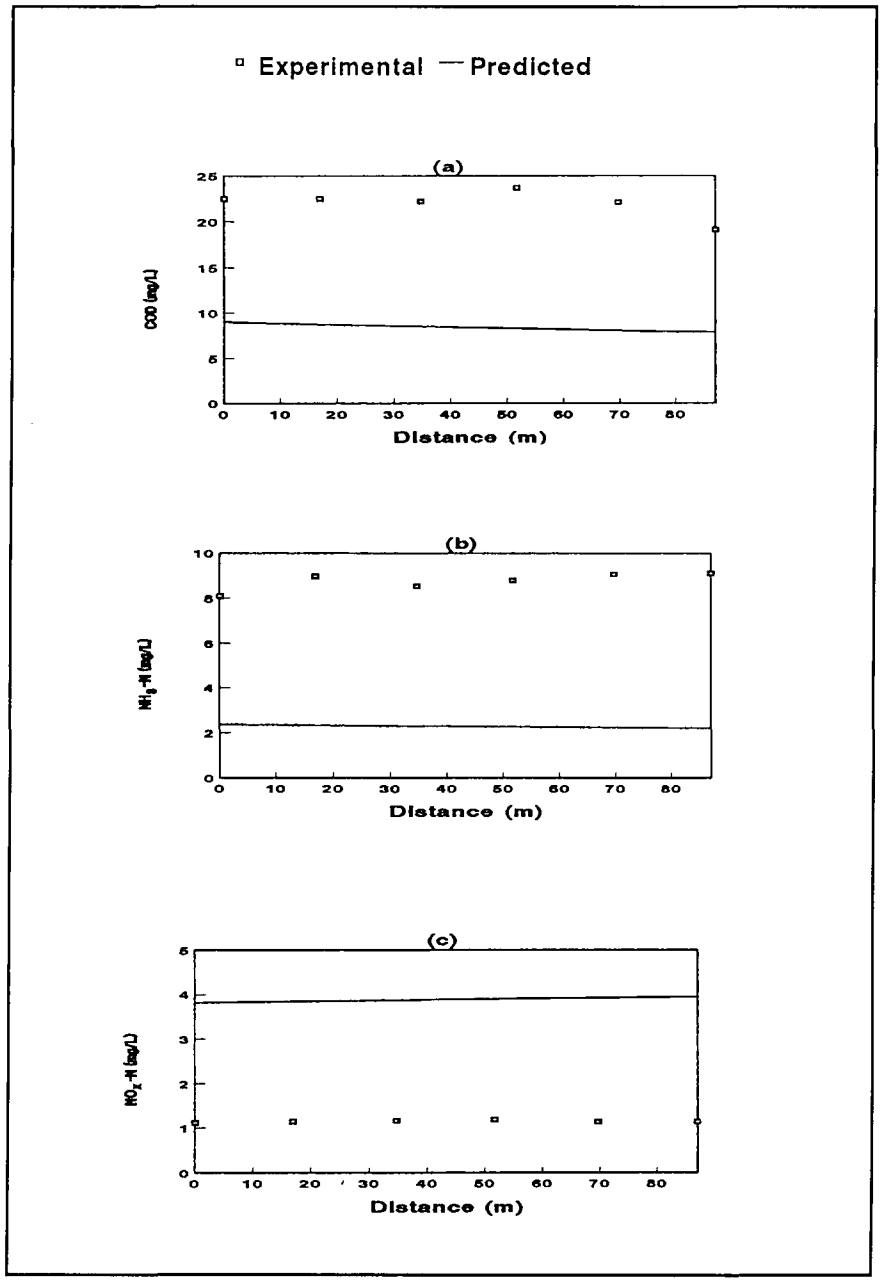

Figure 10. Simulated profiles for Run S3 (a, b, c—with coefficients from Run S2; and d, e, f—with coefficients from Run S4).

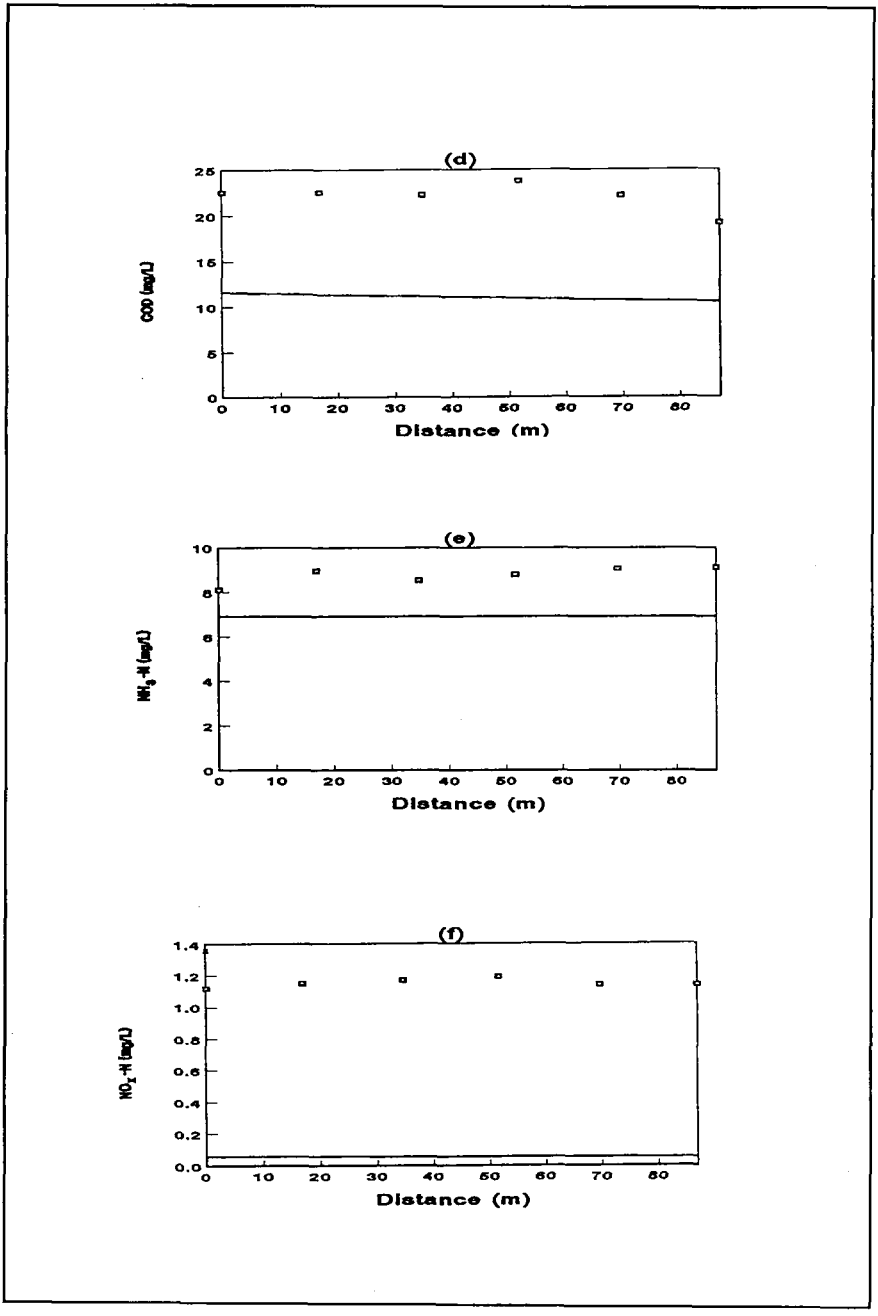

Figure 10. (Cont'd.)

Equations 3a to 3c and mass balance equations for the recirculation tank, the model predicts the contribution of biofilm biomass on COD removal. The COD removal efficiencies from the model simulation for these cases are given in Table 4. It can be seen from Table 4 that both suspended and biofilm biomass were significant at low loadings (i.e., runs S1 and S2) in terms of COD removal efficiency. At higher loadings (runs S4 to S6), the COD removal efficiency by suspended biomass alone was comparatively higher than that by biofilm biomass only. This is due to less growth of heterotrophic bacteria in attached form because of low DO level in the system. However, it could not be checked in terms of TN removal due to the fact that the model does not predict organic nitrogen in the system.

Although the COD removal efficiencies obtained by considering suspended biomass and biofilm biomass separately are less than 100 percent, the sum of these efficiencies is greater than 100 percent and the COD removal efficiency by both biomass (Table 4). This indicates the interaction between these two forms of biomasses in terms of COD removal. The same will be true of other substrates.

CONCLUSION

A mathematical model has been formulated for the Sewage Circulating Reactor by incorporating suspended-growth and attached-growth kinetics. The model

Table 4. COD Removal Efficiency by Suspended and Biofilm Biomass

	Run No.					
Description	S1	S2	S4	S5	S6	Remarks
Percent removal by Suspended Biomass only	74.0	68.6	79.7	93.2	92.0	By setting a = 0 in Equations 3a to 3c
Percent removal by Biofilm Biomass only	73.1	58.4	26.7	21.2	21.5	By setting K_{msn}, K_{msp}, and K_{mss} equal to 0 in Equations 3a to 3c and mass balance eqs. for recirculation tank
Percent removal by combined effect of both Biomass	86.7	80.8	86.4	93.9	93.7	
Observed removal Efficiency	87.4	86.2	86.2	89.2	88.3	

simulated the performance of the system reasonably well; the K_m value being obtained by fitting simulated and experimental profiles. The model simulation indicated that all three biological reactions (carbon oxidation, nitrification, and denitrification) occur simultaneously in the system. However different operating parameters and environmental conditions; including loadings, DO levels, and recycling ratios, are found to affect these processes in the system. The K_m values for carbon oxidation and nitrification were higher for experimental runs with higher DO levels, indicating that lower loadings are favorable for these two processes. Higher loadings (i.e., low DO levels) were found to be suitable for denitrification, thus giving a higher K_m value for denitrification. In terms of organic removal, the model simulation indicated that both suspended and biofilm biomasses were significant at low loadings, and suspended biomass was more significant than biofilm biomass at higher loadings.

NOMENCLATURE

Symbol	Description	Unit
a	Specific surface area	L^{-1}
A_s	Biofilm contact area in channel	L^2
b_1	Decay coefficient for heterotrophs	T^{-1}
b_2	Decay coefficient for nitrifiers	T^{-1}
b_{1d}	Decay coefficient for denitrifying heterotrophs	T^{-1}
C	Concentration of a substrate	ML^{-3}
D_{fn}	Diffusion coefficient of NH_4–4 within biofilm	L^2T^{-1}
D_{fo}	Diffusion coefficient of DO within biofilm	L^2T^{-1}
D_{fp}	Diffusion coefficient of NO_x–N within biofilm	L^2T^{-1}
D_{fs}	Diffusion coefficient of organic substance within biofilm	L^2T^{-1}
D_{wn}	Diffusion coefficient of NH_4–N in diffusion sublayer	L^2T^{-1}
D_{wo}	Diffusion coefficient of DO in diffusion sublayer	L^2T^{-1}
D_{wp}	Diffusion coefficient of NO_x–N in diffusion sublayer	L^2T^{-1}
D_{ws}	Diffusion coefficient of organic substance in diffusion sublayer	L^2T^{-1}
f	Stoichiometric ratio of NH_4–N consumed for cell synthesis	—
f_{oc}	Stoichiometric DO use coefficient for carbon oxidation	MM^{-1}
f_{oa}	Stoiciometric DO use coefficient for nitrification	MM^{-1}
g	Acceleration due to gravity	LT^{-2}
H	Flow depth	L
J_c	Flux of a substrate into biofilm	$ML^{-2}T^{-1}$
J_n	NH_4–N flux into biofilm	$ML^{-2}T^{-1}$
J_p	NO_x–N flux into biofilm	$ML^{-2}T^{-1}$
J_s	Organic substance flux to biofilm	$ML^{-2}T^{-1}$
K_{msn}	Maximum rate of nitrification in bulk liquid	T^{-1}

K_{msp}	Maximum rate of denitification in bulk liquid	T^{-1}
K_{mss}	Maximum rate of carbon oxidation in bulk liquid	T^{-1}
K_{fn}	Saturation coefficient for NH_4–N in biofilm	ML^{-3}
K_{fon}	DO saturation coefficient for nitrification in biofilm	ML^{-3}
K_{fp}	Saturation coefficient for NO_x–N in biofilm	ML^{-3}
K_{fsp}	Organic substance saturation coeff. for denitrification in biofilm	ML^{-3}
K_{fss}	Organic substance saturation coeff. for carbon oxidation in biofilm	ML^{-3}
K_{fos}	DO saturation coefficient for carbon oxidation in biofilm	ML^{-3}
K_{mfn}	Maximum rate of nitrification in biofilm	T^{-1}
K_{mfp}	Maximum rate of denitrification in biofilm	T^{-1}
K_{mfs}	Maximum rate of carbon oxidation in biofilm	T^{-1}
K_{sn}	Saturation coefficient for NH_4–N in bulk liquid	ML^{-3}
K_{son}	DO saturation coefficient for nitrification in bulk liquid	ML^{-3}
K_{sos}	DO saturation coefficient for carbon oxidation in bulk liquid	ML^{-3}
K_{sor}	DO inhibition coefficient of denitrification in bulk liquid	ML^{-3}
K_{sp}	Saturation coefficient for NO_x–N in bulk liquid	ML^{-3}
K_{ssp}	Organic substance saturation coeff. for denitrification in bulk liquid	ML^{-3}
K_{sss}	Organic substance saturation coeff. for carbon oxidation in bulk liquid	ML^{-3}
L_1	Thickness of diffusion layer	L
N	Bulk NH_4–N concentration	ML^{-3}
N_{in}	Influent ammonia concentration	ML^{-3}
$N_e^{\ it}$	Recycle flow NH_3 concentration after it^{th} iteration	ML^{-3}
N^{it+1}	Steady-state NH_3 concentration at point Z for $(it + 1)^{th}$ iteration	ML^{-3}
O	Bulk DO concentration	ML^{-3}
P	Bulk NO_x–N concentration	ML^{-3}
Q	Flow rate	L^3T^{-1}
R	Recycle ratio	—
r_s	Substrate utilization rate by suspended media	$ML^{-3}T^{-1}$
S	Bulk organic substance concentration	ML^{-3}
S_e,N_e,P_e	Effluent COD, NH_3–N and NO_x–N concentrations	ML^{-3}
t	Time	T
U	Flow velocity	LT^{-1}
$\overline{U}$	Depth averaged flow velocity	LT^{-1}
ΔV	Volume under consideration	L^3
W	Width of channel	L
x	Distance along channel	L
X	Suspended biomass density	ML^{-3}

Y_1	Yield coefficient for heterotrophs	MM^{-1}
Y_{1d}	Yield coefficient for denitrifying heterotrophs	MM^{-1}
Y_2	Yield coefficient for nitrifiers	MM^{-1}
β	Stoichiometric COD use coefficient for denitrification	MM^{-1}
υ	Kinematic viscosity of liquid	L^2T^{-1}
θ	Slope of energy grade line	LL^{-1}

Note: Units are expressed in general terms as: L = Length; M = Mass; T = Time.

REFERENCES

1. M. Green, G. Shelef, and A. Messing, Using the Main Sewerage System Main Conduits for Biological Treatment: Greater Tel Aviv as a Conceptual Model, *Water Research, 19*:8, pp. 1023-1028, 1985.
2. R. L. Stoyer, *The Pressure Pipe Wastewater Treatment System,* presented to the 2nd Annual Sanitary Engineering Research Laboratory Workshop on Wastewater Reclamation and Reuse, Tahoe City, California, 1970.
3. C. M. Koch and J. Zandi, Use of Pipelines as Aerobic Biological Reactors, *Journal of Water Pollution Control Federation, 45*, pp. 2537-2548, 1973.
4. U K. Manandhar and H. Schroder, Sewage Circulating Reactor—An Approach to Recirculating Wastewater in Sewers, *Environment Technology Letters, 16*, pp. 201-212, 1995.
5. G. H. Chen, H. Ozaki, and Y. Terashima, Modelling of the Simultaneous Removal of Organic Substances and Nitrogen in a Biofilm, *Water Science and Technology, 21*, pp. 791-804, 1989.
6. V. G. Levich, *Physicochemical Hydrodynamics*, Prentice-Hall, Inc., Englewood Cliffs, New Jersey, 1962.
7. P. Harremoes, Biofilm Kinetics, in *Water Pollution Microbiology*, Vol. 2, R. Mitchell (ed.), Wiley, New York, 1978.
8. U. K. Manandhar, Sewage Circulating Reactor: An Approach to Recirculating Wastewater in Sewers, *Doctoral Dissertation EV-93-2*, AIT, Bangkok, Thailand, 1993.
9. P. B. Saez and B. E. Rittmann, Improved Pseudoanalytical Solution for Steady-State Biofilm Kinetics, *Biotechnology and Bioengineering, 32*, pp. 379-385, 1988.
10. K. J. Williamson and P. L. McCarty, Verification Studies of the Biofilm Model for Bacterial Substrate Utilization, *Journal of Water Pollution Control Federation, 48*:2, pp. 281-296, 1976.
11. K. M. Brown, Computer Oriented Algorithm for Systems of Simultaneous Nonlinear Algebraic Equations, in *Numerical Solution of Systems of Nonlinear Algebraic Equations*, G. D. Byrne and C. A. Hall (eds.), Academic Press, Orlando, Florida, 1973.
12. P. L. McCarty, Stoichiometry of Biological Reactions, *Progress in Water Technology, 7*:1, pp. 157-172, 1975.
13. E. Gonenc and P. Harremoes, Nitrification in Rotating Disc Systems: I Criteria for Transition from Oxygen to Ammonia Rate Limitation, *Water Research, 19*:9, pp. 1119-1127, 1985.

14. Metcalf and Eddy, Inc., *Wastewater Engineering: Treatment, Disposal, Reuse,* McGraw Hill Book Co., New York, 1991.
15. E. Arvin and P. Harremoes, Concepts and Models for Biofilm Reactor Performance, *Water Science and Technology, 22*:1/2, pp. 171-192, 1990.
16. S. Jayamohan, S. Ohjaki, and K. Hanaki, Effect of DO on Kinetics of Nitrification, *Water Supply, 6*, Brussels, pp. 141-150, 1988.
17. J. E. Alleman, Elevated Nitrite Occurrence in Biological Wastewater Treatment Systems, *Water Science and Technology, 17*, pp. 409-419, 1984.

Direct reprint requests to:

Uttam K. Manandhar
Seatec International
P.O. Box 8-101
Bangkok 10800
Thailand